




Development and characterization of edible bilayer films based on iron yam–pea starch blend and corn zein

Xiaoyong SONG^{1*} , Yiqi WANG¹

Abstract

We prepared bilayer films of iron yam–pea starch and corn zein to evaluate their potential application in the packaging of instant foods and condiments. We found that the water resistance and mechanical properties of bilayer films were improved after adding a layer of corn zein compared with the monolayer films of the starch materials. Scanning electron microscopy revealed that the bilayers were close and this was reflected in increased thermal stability and biocompatibility between layers with the addition of zein. Our experimental films showed greater elongation at break than the commercial biaxially oriented polypropylene polyethylene films. Based on the results of this study, the iron yam-pea starch/corn zein films have the mechanical strength and flexibility to be used for convenience food packaging materials, which are expected to provide consumers with clean products.

Keywords: iron yam-pea starch; corn zein; bilayer edible film; microstructure; thermal properties; food inner packaging.

Practical Application: Provide a degradable bilayer edible film used as convenient food seasoning packaging material.

1 Introduction

The convenience food industry has entered a period of rapid growth (Song et al., 2018b) due to changing trends in consumer lifestyles but this has also resulted in problems associated with waste and disposal of packaging materials (Koshy et al., 2015; Song et al., 2018a). The packaging including bags and wraps for these foods are constructed of plastic films using polyethylene such as biaxially oriented polypropylene polyethylene composite film (BOPP) and other PE films. However, these types of plastics cannot be recycled with other plastics and are not biodegradable. Moreover, incineration of these materials produces dioxins and other harmful substances that are health and environmental threats (Cao et al., 2018; Turner, 2018). Additionally, these types of plastic packaging are often not easy to open leading to spills, difficulties in extruding the material and this increased the chance for microbial contamination. Plastic films only provide limited protection from oxygen, and oil condiments in packaging are vulnerable to lipid oxidation resulting in unpleasant odors and potentially toxic by-products such as malondialdehyde, glyoxal and acetone aldehyde. Direct contact between oil and plastic packaging can also result in plasticizer transfer to fat-rich seasonings that have their own health risks (Hahladakis et al., 2018). If the traditional plastic packaging is replaced by edible materials, edible condiment bags and food can be eaten together directly after being brewed in hot water and are one solution to the myriad of problems posed by packaging food in plastic films (Soo & Sarbon, 2018).

There have been numerous studies on the production of biodegradable or edible packaging materials (Brink et al., 2019; Leonardo & Jonas, 2020; Santoso et al., 2019; Wang et al., 2019). For instance, edible bilayer films have been produced from grey triggerfish gelatin-agar (Jridi et al., 2019), corn distarch

phosphate-zein (Sun et al., 2018), gelatin-polyethylene (Nur Hanani et al., 2018), polyvinyl alcohol-chitosan-alginate (Zhuang et al., 2018), poly-materBi (Scaffaro et al., 2018), chitosan-gelatin (Haghighi et al., 2019), polylactic acid-Pickering emulsions (Zhu et al., 2018), chitosan-polycaprolactone (Sogut & Seydim, 2018), fish gelatin-poly (Nilsuwan et al., 2018), cassava starch-chitosan (Valencia-Sullca et al., 2018), chitosan–sodium alginate (Wang et al., 2019). These edible bilayer films have been proven to keep fruit and vegetables fresh including sweet cherry (Xin et al., 2020), apricot (Zhang et al., 2018), citrus fruit (Arnon et al., 2014) and walnuts (Ferreira et al., 2018). These materials have also been used for shrimp (Arancibia et al., 2014), chicken breast fillets (Sogut and Seydim, 2019), olive oil (Cho et al., 2010), chicken skin oil (Nilsuwan et al., 2019). A biodegradable film has also been produced as a wound dressing (Thu et al., 2012). To the best of our knowledge, there edible bilayer films based on iron yam starch, pea starch and corn zein have not been attempted.

The iron yam (*Dioscorea opposita* Thunb) is named for its rusty red spots on the epidermis. It is grown primarily in Jiaozuo City, Henan Province, China and is the only yam species that is protected under the national origin protection list in China (Zhang et al., 2016). The iron yam has been used as a food source since ancient times and has a starch content as high as 28% and a waxy taste. The objective of this study was to prepare iron yam-pea starch/corn zein bilayer films with properties suitable for the production of packaging materials. The effects of corn zein content on the physical and chemical properties (thickness, moisture content, water resistance, swelling, tensile strength, elongation at break and puncture strength) of bilayer films were investigated. We also examined the thermodynamic and microstructural properties of bilayer films in order to

Received 23 July, 2020

Accepted 17 Sept., 2020

¹North China University of Water Resources and Electric Power, Zhengzhou, China

*Corresponding author information: songxiaoyong@ncwu.edu.cn

evaluate their potential performance when used in edible inner packaging for instant foods.

2 Materials and methods

2.1 Materials

Iron yam (*D. opposita*) starch was provided by Hangzhou Mei Yan Trade (Hangzhou, China). Pea starch was provided by Shanghai Luyuan Starch (Shanghai, China) and corn zein (CZ, 91.1% protein content) was provided by Dulai Biotechnology (Nanjing, China). D-Sorbitol ($\geq 98.0\%$), citric acid ($\geq 99.5\%$), absolute ethyl alcohol ($\geq 99.7\%$), polyethylene glycol-400 ($\geq 99.0\%$) and glycerol ($\geq 99.0\%$) were supplied by Tianjing Chemical Reagent (Luoyang, China). Biaxially oriented polypropylene polyethylene composite films (BOPP) were commercially obtained from Henan Nanjiecun, Henan, China. All other chemicals from local resources were of analytical grade.

2.2 Film preparation

The bilayer films were designed by adding a corn zein layer on a dried iron yam-pea starch film (IYP). In brief, the starch film forming solution (6% w/v) was prepared by dissolving iron yam and pea starch at a 2:3 (w/w) ratio in distilled water and adding sorbitol (0.6% w/v), citric acid (2.5% w/v). Sorbitol and citric acid were added as plasticizers that have direct effects on the mechanical properties of films. The mixture was then stirred for 20 min at 40 °C. Starch gelatinization was then induced by heating the mixture at 85 °C for 40 min and that was then degassed for 30 min under a vacuum of 0.09 Pa at 80 °C. The IYP film layer was first formed by casting the starch film forming solution on 100 mm diameter plastic dishes that were then dried at 45 °C for 12 h. The protein film forming solution was prepared by dissolving 6.00 g corn zein in 100 mL 95% ethanol and stirring for 3 min. Different proportions of CZ were added to the basal starch mixture and 5 different formulas were used (Table 1). Polyethylene glycol (PEG) 400 (0.90 g) and glycerol (1.80 g) were added as plasticizers into the solution and stirred for 20 min followed by incubation for 18 min at 80 °C. The mixture was cooled to 45-55 °C and poured onto a dried IYP film in a plastic dish and allowed to dry at room temperature for 30 min and

then at 80 °C for 30 min. The films were then conditioned to 54% relative humidity within a desiccator at room temperature for 2 d. All films were prepared in triplicate.

2.3 Thickness, water content, film solubility, water vapor permeability

Film thickness was measured in five places using a GM280F thickness gauge (Shenzhen Huaqing Instrument, Shenzhen, China) to an accuracy of 0.01 μm . One of the measuring places was the center of the film, the remaining four measuring places were selected in the outer edges, and average values were used. Eight replications of each formulation have been made.

Water content (WC) was measured before and after dried in an oven at 105 °C for 24 h. WC was calculated as the following equation (Equation 1) (Song et al., 2018a):

$$WC = (M_0 - M) / M_0 \quad (1)$$

Where M_0 -the initial mass (g), M-the bone-dry mass (g). WC was expressed as g H_2O /g dry solids. Measurements were repeated 3 times.

The swelling degree (SD) and water solubility (WS) of the films were determined as previously described (Silva et al., 2009). The film sample (20×20 mm) was placed in a dryer containing P_2O_5 for 7 days, and the initial mass M_1 of the film was obtained. Then the film sample was placed in a 100 mL beaker containing 80 mL distilled water, sealed with plastic film, and placed in the mouth of the beaker to absorb water adequately at 25 °C. After 24 hours, the surface water of the film was wiped off with filter paper and the mass was recorded as M_2 . After that, the film samples were removed into a dryer containing P_2O_5 and placed for 7 days to determine the final mass M_3 . Each group of film was repeated three times. SD and WS were calculated according to the following formulas (Formulas 2 and 3) (Silva et al., 2009):

$$SD = (M_2 - M_1) \times 100\% / M_1 \quad (2)$$

$$WS = (M_1 - M_3) \times 100\% / M_1 \quad (3)$$

Water vapor permeability (WVP) was measured gravimetrically according to the modified method previously described (Song et al., 2018a). The thickness of each film was measured by a micrometer at five randomly selected points. The films were sealed onto permeation cells (1384.74 $\text{mm}^2 \times 25$ mm) filled with granular ($\Phi < 2\text{mm}$) anhydrous calcium chloride. The permeation cells were then placed in desiccators filled with saturated sodium chloride solutions at relative humidity (RH) of 0, 75 and 100% at 25 °C and were weighed until weight changes were close to 0.001 g. WVP was calculated use the following equation (Equation 4) (Song et al., 2018a):

$$WVP = mL / (At\Delta P) \quad (4)$$

Table 1. Basic components of test films.

Sample	Description
IYP10/CZ0	10 mL iron yam-pea starch forming solution with 0 mL corn zein solution*
IYP10/CZ1	10 mL iron yam-pea starch forming solution with 1 mL corn zein solution
IYP10/CZ2	10 mL iron yam-pea starch forming solution with 2 mL corn zein solution
IYP10/CZ3	10 mL iron yam-pea starch forming solution with 3 mL corn zein solution
IYP8/CZ0	8 mL iron yam-pea starch forming solution with 3 mL corn zein solution
BOPP-PE	Biaxially oriented polypropylene polyethylene composite films

Where: m (g), L thickness (m), A permeation area (m^2), t (s), ΔP water vapor pressure difference (Pa). Each material type was tested 5 times.

2.4 Mechanical properties

A TA-XT2i Texture Analyzer (Stable Microsystems, Godalming, UK) was used to measure the tensile properties as previously described (Song et al., 2018a). The edible films were cut into 20×80 mm rectangles and fixed between the tensile grips. Initial grip separation was 60 mm and crosshead speed was 1.0 mm s^{-1} . Tensile strength and elongation at break were used to evaluate the mechanical properties. Each sample type was tested 9 times.

2.5 Thermogravimetric Analysis (TGA)

Thermogravimetric tests were performed using a TGA Q500-O574 instrument (TA Instruments, New Castle, PA, USA) as previously described (Gutiérrez et al., 2015). 10 mg samples were heated from 40 to 500 °C at a rate of 10°C/min under a flow of N_2 gas at 30 mL/min. Material weight loss was recalculated on a dry basis and the different degradation phases noted. Analyses were performed in triplicate to ensure repeatability.

2.6 Differential Scanning Calorimetry (DSC)

Differential scanning calorimetry was performed using a DSCSTA-449C instrument (Netzsch, Selb, Germany) as previously described (Nilsuwan et al., 2018). Temperature calibration was performed using the indium thermogram. A sample weight of approximately 5 mg was packed and sealed in a high pressure aluminum pan using an empty aluminum pan as reference. The heating of the samples was performed in the range of 25–250 °C at a constant heating rate of 10 °C/min. The maximum transition temperature of the material was estimated by the endothermic peak of DSC temperature spectrum and the transition enthalpy determined by the area under the endothermic peak. The test was performed in 5 times for each sample type.

2.7 X-ray Diffraction (XRD)

X-ray diffraction (XRD) of the film was obtained from a D8 X-ray diffractometer (Brooke AXS, Berlin, Germany) at 25 °C. It was equipped with a copper tube operating at 40 kV and 30 mA, a 1° divergence slit, a 1° scatter slit and a 0.3 mm receiving slit. XRD patterns were recorded in an angular range of 5–60° (2θ) with scanning rate of 4° min^{-1} .

2.8 Fourier Transform Infrared spectra (FTIR)

Fourier transform infrared (FTIR) spectra of the films were measured using a Nicolet iS50 instrument (Thermo, Pittsburgh, PA, USA) in total reflection mode. The spectra were obtained at a 4 cm^{-1} resolution and averaged over 32 scans in the range of 4000–650 cm^{-1} .

2.9 Scanning Electron Microscope (SEM)

A Quanta FEG 250 field emission scanning electron microscope (FEI, USA) operating at 3 kV was used to analyze film microstructures. The samples were conditioned by exposure to P_2O_5 at 25 °C with 0% relative humidity for 2 weeks. The samples were then cut into 50×60 mm pieces and fractured by immersion in liquid nitrogen. Samples were mounted on metal grids using double-sided adhesive tape and coated with gold under vacuum.

2.10 Statistical analysis

Analysis of variance was performed by ANOVA procedures of the SPSS software (version 16.0 (IBM, Chicago, Ill, USA)). The LSD test was used to determine the difference of means and $P < 0.05$ was considered statistically significant.

3 Results and discussion

3.1 Thickness, water content, solubility and water vapor permeability

An ideal biodegradable film for packaging would have to be thin enough to be flexible without tearing and be relatively water impervious. Thickness, water content, solubility and water vapor permeability of the films were measured (Table 2). We produced a series of film thicknesses by altering the proportion of zein added to the basal starch paste. The thickness of the bilayer film increased by approximately 10 μm with the successive additions of corn zein to the starch preparation. The water content also increased as the proportion of zein was increased whereas the water vapor permeability coefficient decreased. This was an effect of the large number of hydrophobic amino acids in the zein proteins (Cho et al., 2010). The degree of swelling and water solubility also decreased with an increase in zein content and reached minimums in the IYP8/CZ3 film at 128.62 and 34.99%, respectively. These properties were inversely proportional to the water content and resistance because swelling and solubility are related to hydrophobicity (Mathew et al., 2006).

3.2 Mechanical properties

We then examined the mechanical properties of our experimental films to determine whether they would be strong and flexible enough to act as packaging material. The tensile strength was significantly decreased ($P < 0.05$) and elongation at break was significantly increased ($P < 0.05$) as the zein proportion was increased (Table 3). The moisture content affected the mechanical properties of the films and although the tensile strength was less than for BOPP, it still met the requirements for packaging (Cho et al., 2010). The elongation at break of our experimental films was better than BOPP and we found no significant difference between the IYP10/CZ3 and IYP8/CZ3 films in tensile strength and elongation to break. However, an increase in the proportion of zein added resulted in an increase in penetration force that was maximal for IPY10/CZ3 and penetration deformation was maximal for IPY10/CZ0 (Table 3). The effect of corn zein content on the penetration and deformation of bilayer film was different from the tensile

Table 2. Physicochemical properties of the bilayer films.

Films	Thickness (μm)	WC (%)	WVP $10^{-11}(\text{g/m s Pa})$	SD (%)	WS (%)
IYP10/CZ0	115.67 \pm 1.53b	11.80 \pm 0.33a	8.89 \pm 0.02c	137.33 \pm 0.33e	36.97 \pm 0.24c
IYP10/CZ1	126.67 \pm 1.53bc	11.41 \pm 0.26a	6.15 \pm 0.13b	135.33 \pm 0.55d	36.61 \pm 0.31bc
IYP10/CZ2	135.33 \pm 9.29cd	12.95 \pm 0.57a	6.17 \pm 0.66b	132.56 \pm 0.70c	36.55 \pm 0.66bc
IYP10/CZ3	147.00 \pm 0.81d	15.48 \pm 1.22b	5.55 \pm 0.53b	130.17 \pm 0.56b	35.91 \pm 0.71b
IYP8/CZ3	126.67 \pm 3.21bc	12.94 \pm 0.21a	5.31 \pm 0.05b	128.62 \pm 0.64a	34.99 \pm 0.43a
BOPP-PE	60.97 \pm 0.75a	ND	0.31 \pm 0.00a	ND	ND

ND: not determined.

Table 3. Mechanical properties of the bilayer films.

Films	Tensile strength (MPa)	Elongation at break (%)	Penetration force (N)	Penetration deformation (mm)
IYP10/CZ0	15.20 \pm 0.88c	41.70 \pm 1.63a	3.23 \pm 0.17a	11.05 \pm 0.31c
IYP10/CZ1	14.58 \pm 0.27c	54.45 \pm 2.50b	4.82 \pm 0.47b	8.02 \pm 0.48ab
IYP10/CZ2	12.58 \pm 0.75b	64.86 \pm 0.81c	5.20 \pm 0.10b	7.07 \pm 0.40ab
IYP10/CZ3	9.62 \pm 0.13a	75.13 \pm 9.18d	5.77 \pm 0.31c	6.52 \pm 0.57a
IYP8/CZ3	9.16 \pm 0.09a	79.11 \pm 7.43d	5.86 \pm 0.15c	7.32 \pm 0.59bc
BOPP-PE	84.56 \pm 0.39d	42.54 \pm 1.34a	18.62 \pm 0.11d	8.19 \pm 0.04d

strength and elongation at break. This was primarily the result of the different action modes used for testing these variables.

3.3 Thermodynamic properties

Another property that is necessary for a useable film packaging is its thermal stability. We measured the temperatures corresponding to maximum mass loss and rate of mass loss rate by R and T_p (Figure 1), respectively. The mass lost from the films were clearly separated into three to four phases. The first occurred near 100 °C with mass loss primarily derived from free and bound water. The T_{p1} of the zein monolayer film was 58.08 °C and was the result of surface water adsorption due to the particular amino acid composition and was consistent with its water loss. The second stage occurred near 200 °C and was the result of small molecule decomposition including the sorbitol and citric acid used for the production process. The mass loss for the yam and pea starch films ranged from 4.54 to 6.48% and were significantly less than the bilayer films due to the absence of plasticizers that account for ~37% of the bilayer films. However, the new hydrogen bonds and other forces formed using plasticizers resulted in their strong retention in the film matrices. The mass loss rate of the zein monolayer was 20.61% at this stage. This was most likely the result of the water holding capacity of PEG-400 (Mendes et al., 2016). The third and fourth stages occurred at 240 °C and 250 °C, respectively. This was the result of amylose and amylopectin decomposition, respectively. These differing rates were the result of a greater degree of hydroxyl group exposure for amylose and was more conducive to thermal degradation (López et al., 2015; Yalçınkaya & Çakmak, 2017).

These data indicated that of the thermal stability of the iron yam-pea starch and iron yam-pea starch composite films were almost the same. This was indicative of a good blending

between the two biological macromolecules. As we increased the zein content, T_{p2} , T_{p3} and T_{p4} increased from 9.3, 9.0 and 1.0%, respectively, indicating that zein increased the thermal stability of the bilayer films. However, the mass loss rate increased from 71.63 to 76.92% and was inconsistent with the previous analysis results (T_{p2} , T_{p3} and T_{p4}). This might be due to the inherent characteristics of corn zein film that displayed a mass loss of 89.38% at T_{500} . The addition of zein resulted in mass loss rate decreases for R_{13} from 19.39 to 11.03% while R_{14} increased from 33.98 to 45.00%. This was most likely the result of the glycerol and PEG-400 in the protein film-forming solution entering the starch composite film producing amorphous amylose. The hydrogen bonding and other forces altered the crystallinity of the film material and amylose easily formed an amorphous zone in the film material.

This TGA analysis focused on the chemical alterations in the film materials during heating but film material quality does not a priori suffer when biophysical changes such as glass transition occur during heating. In contrast, DSC analysis can be used identify thermorheological changes during heating. We identified two distinct endothermic peaks for our starch-based films at 107-171 °C and 186-210 °C. The first peak most likely represents melting of starch microcrystals while the second peak signifies small molecule decomposition (Wang et al., 2017). The position of the second endothermic peak shifted to the right as the proportion of zein was increased, consistent with TGA analysis. The DSC curves for zein films indicated that the initial, peak and termination temperatures were 128.6, 142.5 and 169.2°C, respectively, indicating that corn zein films had relatively good thermoplasticity (Figure 2).

In contrast, the first endothermic peaks for yam and pea starch films and the composite film did not shift significantly.

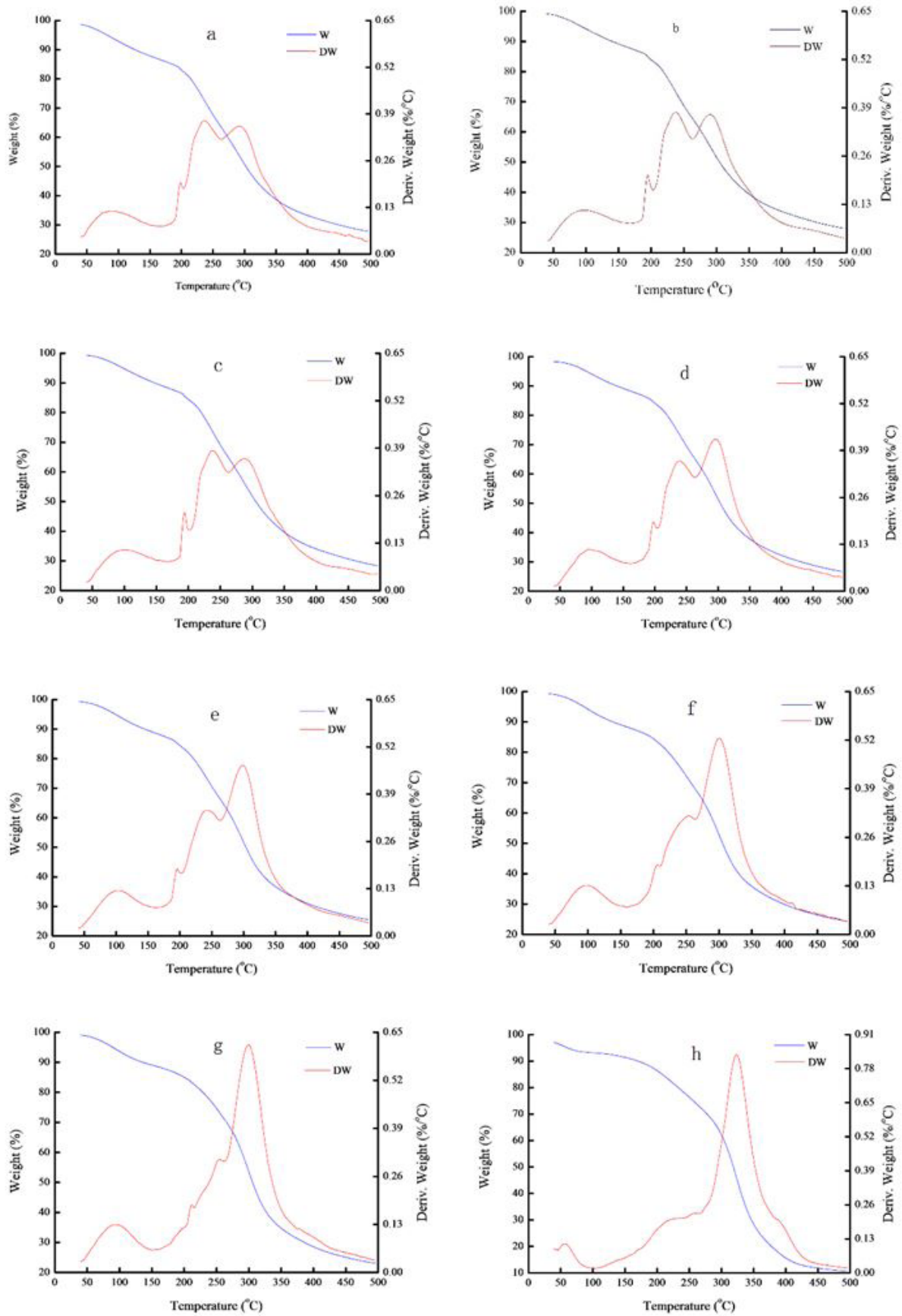


Figure 1. TGA analysis of experimental films formed using different materials. (a). Iron yam starch (b). Pea starch (c). IYP10/CZ0 (d). IYP10/CZ1 (e). IYP10/CZ2 (f). IYP10/CZ3 (g). IYP8/CZ3 (h). Corn zein film. See Table 1 for abbreviations.

The corresponding enthalpy values decreased from -139.5 and -100.8 J/g to -87.03 J/g that represents an alteration in crystallinity (Figure 2a-c) (Shahbazi et al., 2017). The first endothermic peaks for the bilayer films were 143.7, 134.5, 137.6 and 140.4°C, respectively, indicating an improvement in their thermal stabilities. In contrast, small additions of zein i.e. IYP10/CZ1 and IYP10/CZ2 resulted in irregular bilayer films (Figure 2d-g). This might be due to the complex interaction between bilayer films that altered the thermodynamic properties (López et al., 2015).

3.5 Alterations in internal structure

Thermal property measurements are also a reflection of the internal crystalline structure of the material. We therefore used x-ray diffraction to more closely examine alterations in the

crystalline state of the experimental films. The XRD spectra of the starch-based film materials showed wide diffraction peaks indicative of semi-crystalline polymers as a result of destruction of the starch double helical structure and an accompanying crystallinity decrease during the gelatinization step of manufacture (Lopez et al., 2014). We found a significant diffraction peak at 20° and a weak at 17° for the yam and pea starch materials. The 17° peak indicated B-type crystal formation and we found no evidence of A-type crystals that further confirmed that the gelatinization process had changed the starch granule structure (Mendes et al., 2016) (Figure 3a and b). In contrast, the yam-pea composite film lacked the 17° peak and crystallinity decreased from 53.99 and 60.23 to 47.85% for the composite (Figure 3c). This indicated that there was a good biocompatibility between the two macromolecules in the iron yam-pea starch composite film

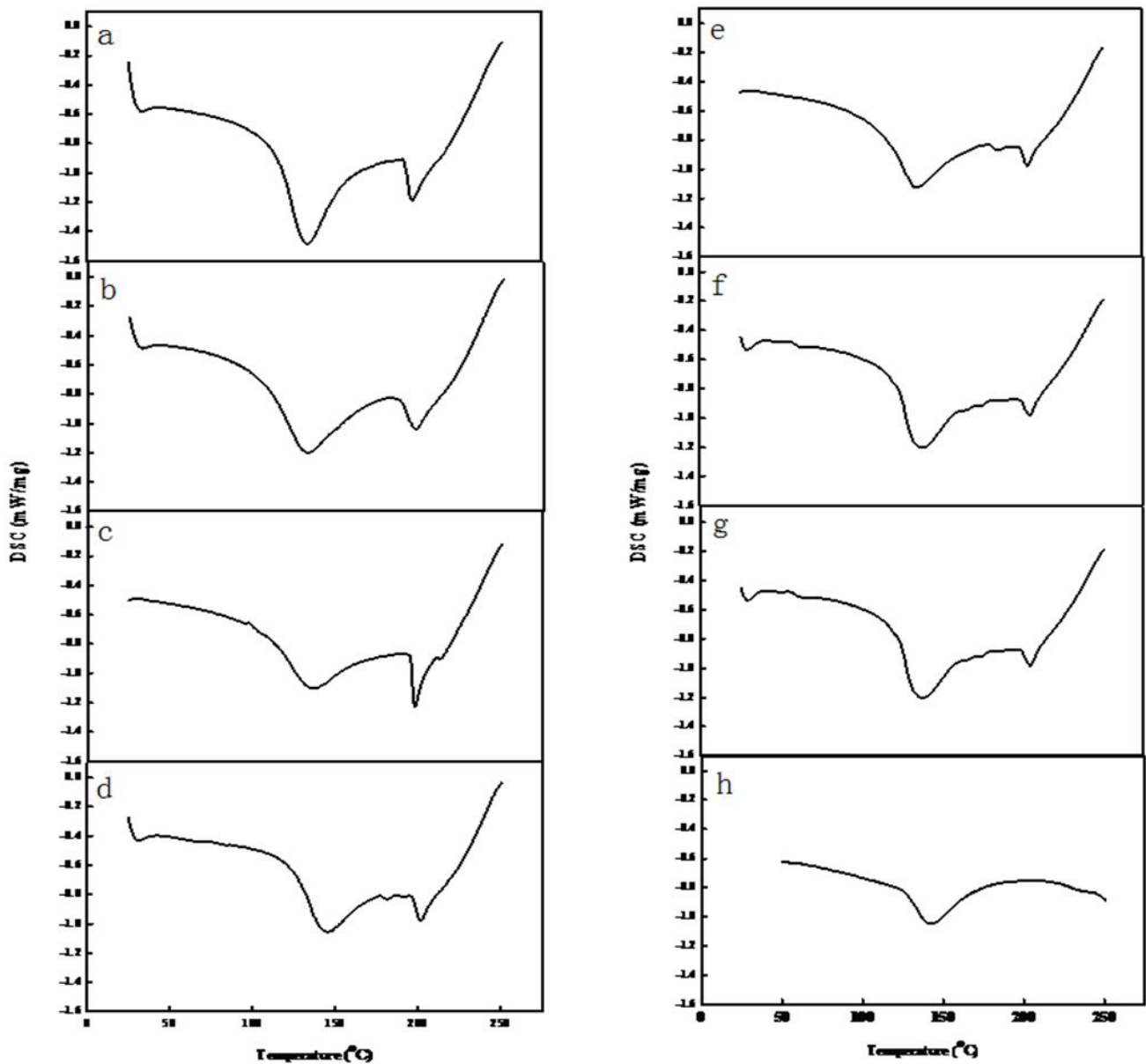


Figure 2. DSC analysis of experimental films (a). Iron yam starch film (b). Pea starch film (c). IYP10/CZ0 (d). IYP10/CZ1 (e). IYP10/CZ2 (f). IYP10/CZ3 (g). IYP8/CZ3 (h). Corn zein film. See Table 1 for abbreviations.

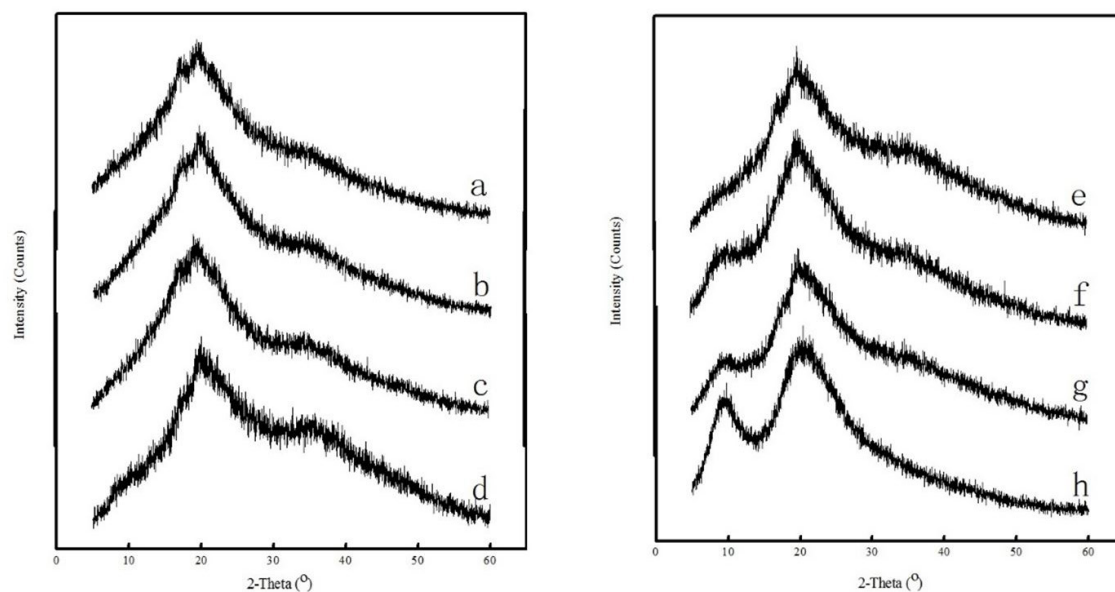


Figure 3. XRD analysis of experimental films (a). Iron yam starch film (b). Pea starch film (c). IYP10/CZ0 (d). IYP10/CZ1 (e). IYP10/CZ2 (f). IYP10/CZ3 (g). IYP8/CZ3 (h). Corn zein film. See Table 1 for abbreviations.

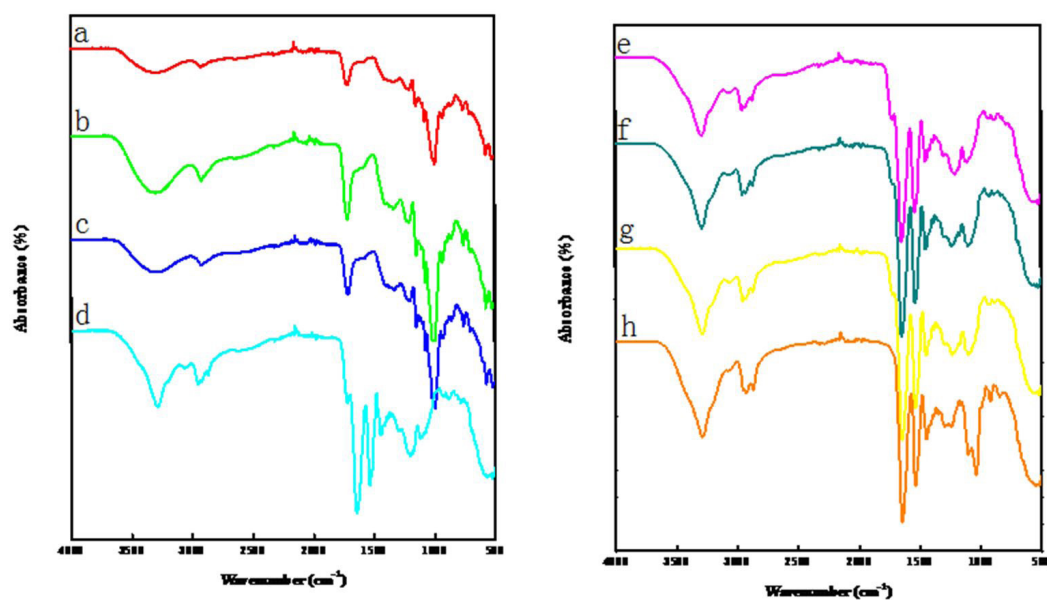


Figure 4. FTIR analysis of experimental films (a). Iron yam starch film (b). Pea starch film (c). IYP10/CZ0 (d). IYP10/CZ1 (e). IYP10/CZ2 (f). IYP10/CZ3 (g). IYP8/CZ3 (h). Corn zein film. See Table 1 for abbreviations.

(Ren et al., 2017) and was consistent with our thermodynamic analyses. The addition of zein resulted in diffraction peaks at 9.5° and 21° and was consistent with previous results (Escamilla-García et al., 2013) (Figure 3d-h). The crystallinity of corn zein films reached 58.79% and was most likely resulted from full exposure of lysine β -amino and cysteine -SH groups during heat treatment. In addition, hydrogen bonding with PEG-400 and glycerol made the internal structure more orderly and uniform. Therefore, the overall elongation at break of the bilayer films increased with the addition of a layer of zein film.

We also found no characteristic diffraction peaks for the zein film samples IYP10/CZ1 and IYP10/CZ2 indicating

that the hydrogen bonding between bilayer films had limited crystallization. However, with a further increase in zein content (IYP10/CZ3 and IYP8/CZ3), a 9.5° diffraction peak appeared as well as at $19\text{--}20^\circ$. This difference indicated that the alteration in crystal structure not only affected the thermal properties but also indirectly reflected the changes of the internal molecular structure of the films.

To examine this further we used FTIR to analyze alterations in molecular interactions. The addition of zein resulted in a stretching of the O-H (3296 cm^{-1}) and this peak was shifted to the right for IYP10/CZ1: 3288 cm^{-1} , IYP10/CZ2: 3289 cm^{-1} , IYP10/CZ3: 3289 cm^{-1} and IYP8/CZ3: 3288 cm^{-1} (Figure 4).

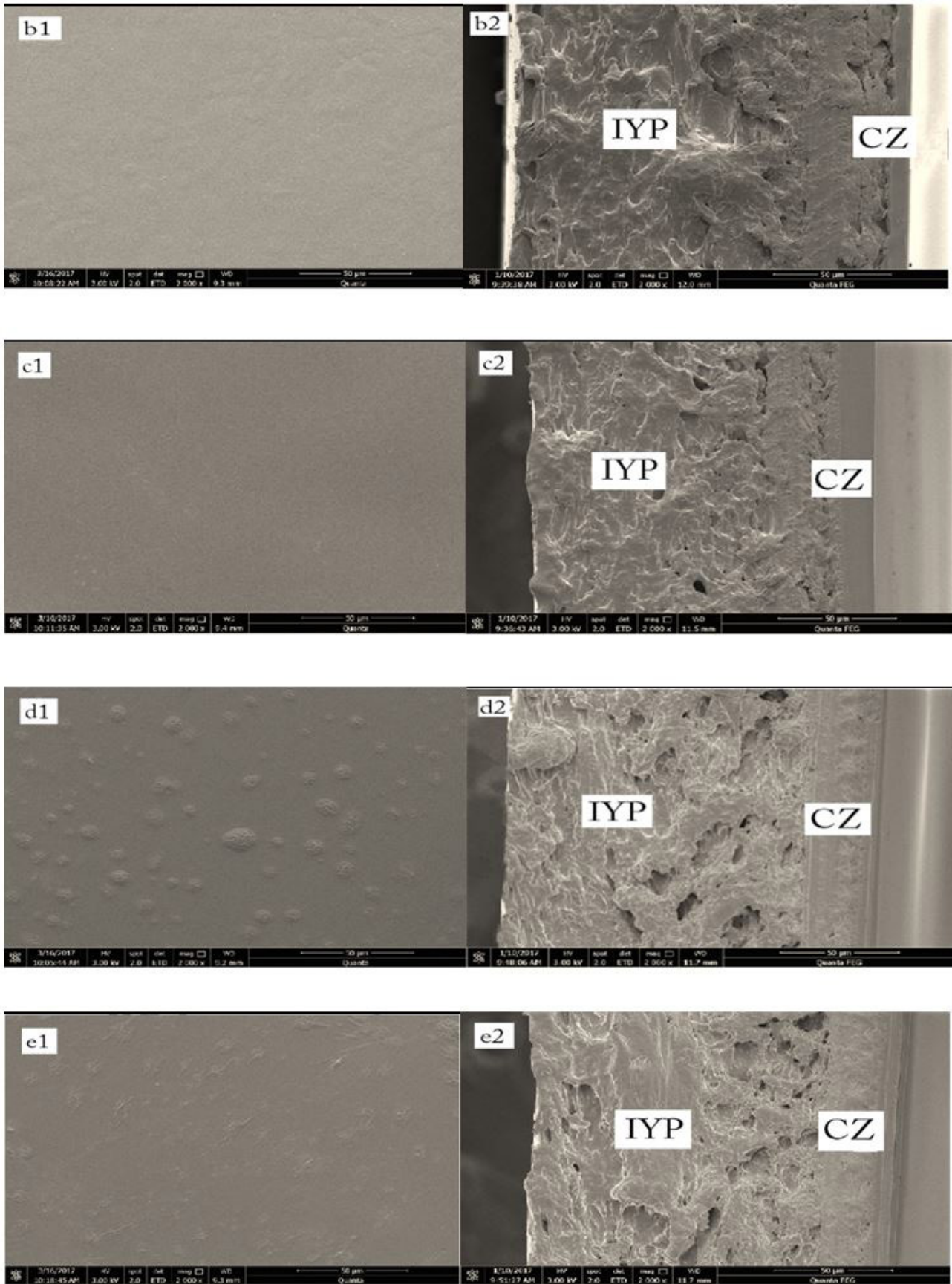


Figure 5. SEM micrographs of experimental films (a). IYP10/CZ0 (b). IYP10/CZ1 (c). IYP10/CZ2 (d). IYP10/CZ3 (e). IYP8/CZ3. Surface images (left) and cross sectional images (right) for the indicated formulas. Magnification 2000 \times . See Table 1 for abbreviations.

These correlated with increased film strength and the IYP10/CZ1 film was most significantly altered. This might be indicative of new hydrogen bonds and other forces that formed by the introduction of glycerol and PEG-400 or the hydrogen bonds between starch hydroxyls and protein amino groups that increased the interaction forces (Castillo et al., 2013) (Figure 4). These conclusions are consistent with DSC analysis (Figure 2). The starch films had characteristic absorption peaks for polysaccharides at 1200-800 cm^{-1} . The introduction of proteins caused new absorption peaks at 1644 cm^{-1} (amide I region: C=C bond stretching vibration), 1537 cm^{-1} (amide II region: N-H bond bending) and 1447 cm^{-1} (amide III region). With increased corn zein content, the vibration peak of the bilayer film at 1720 cm^{-1} (carboxylic acid C=O) fluctuated and gradually disappeared. This might be due to the chemical interaction between carbonyls that further indicated that there was a good compatibility between biological macromolecules. At the same time, the starch -COOH groups could esterify with the ethanol -OH group present in the corn zein solvent. These are also indicative of electrostatic attractions between bilayer films (Ninago et al., 2015). Additionally, the peak shapes at 1332-1234 cm^{-1} increased in complexity as the zein content was increased indicating polysaccharide-protein interactions as had been previously demonstrated (Liang et al., 2017). The peak at 880 cm^{-1} in the fingerprint region became stronger indicating the presence of new C-C bonding (Figure 4). The corn zein also introduced a large number of hydrophobic amino acids into the composites that might allow hydrophobic interactions between bilayer films.

3.7 Surface and cross sectional analysis

Our experimental films were also examined microscopically using SEM in surface and cross sectional views. The surface of the iron yam-pea starch composite film IYP10/CZ0 appeared rough. The addition of zein altered this morphology to smooth with significant decreases in the concave and convex morphologies of IYP10/CZ1 and IYP10/CZ2 films. In contrast, the further increase in zein content resulted in bulges for IYP10/CZ3 and IYP8/CZ3 films at the surface level (Figure 5a-e, left panels). This was most likely due to zein aggregation in the presence of 95% ethanol (Soliman et al., 2014). In cross section, the densities were poor for the starch only film. In contrast, the binding between bilayer films was close and lacked any evidence of separation and the IYP10/CZ3 and IYP8/CZ3 produced a transition zone (Figure 5a-e, right panels).

4 Conclusions

We examined the effects that the addition of corn zein to iron yam-pea starch had on bilayer films. We found that adding a layer of corn zein to IYP bilayer films improved their mechanical properties and increased the water content, resistance, degree of swelling and solubility. In addition, the bilayer films IYP10/CZ1, 2 and 3 and IYP8/CZ3 showed better elongation at break than the commercial film BOPP. An increase in corn zein content improved the thermal stabilities of the films and resulted in better compatibility between bio-macromolecules and better crystal structures. We also found that intermolecular bonding

between bilayers was increased with zein addition. These results suggest that iron yam-pea starch/corn zein bilayer films could be used as a choice of edible packaging materials, especially convenient food packaging.

Acknowledgments

This work was funded by the Training Plan of Young Key Teachers in Colleges and Universities of Henan Province (2018131), the Training Plan of Young Key Teachers of North China University of Water Resources and Electric Power (2018176), the Youth Science and Technology Innovation Talents Support Program of North China University of Water Resources and Electric Power (70442).

References

- Arancibia, M., Giménez, B., López-Caballero, M. E., Gómez-Guillén, M. C., & Montero, P. (2014). Release of cinnamon essential oil from polysaccharide bilayer films and its use for microbial growth inhibition in chilled shrimps. *Lebensmittel-Wissenschaft + Technologie*, 59(2), 989-995. <http://dx.doi.org/10.1016/j.lwt.2014.06.031>.
- Arnon, H., Zaitsev, Y., Porat, R., & Poverenov, E. (2014). Effects of carboxymethyl cellulose and chitosan bilayer edible coating on postharvest quality of citrus fruit. *Postharvest Biology and Technology*, 87, 21-26. <http://dx.doi.org/10.1016/j.postharvbio.2013.08.007>.
- Brink, I., Šipailienė, A., & Leskauskaitė, D. (2019). Antimicrobial properties of chitosan and whey protein films applied on fresh cut turkey pieces. *International Journal of Biological Macromolecules*, 130, 810-817. <http://dx.doi.org/10.1016/j.ijbiomac.2019.03.021>. PMID:30840870.
- Cao, L., Liu, W., & Wang, L. (2018). Developing a green and edible film from Cassia gum: The effects of glycerol and sorbitol. *Journal of Cleaner Production*, 175, 276-282. <http://dx.doi.org/10.1016/j.jclepro.2017.12.064>.
- Castillo, L., López, O., López, C., Zaritzky, N., García, M. A., Barbosa, S., & Villar, M. (2013). Thermoplastic starch films reinforced with talc nanoparticles. *Carbohydrate Polymers*, 95(2), 664-674. <http://dx.doi.org/10.1016/j.carbpol.2013.03.026>. PMID:23648028.
- Cho, S. Y., Lee, S. Y., & Rhee, C. (2010). Edible oxygen barrier bilayer film pouches from corn zein and soy protein isolate for olive oil packaging. *Lebensmittel-Wissenschaft + Technologie*, 43(8), 1234-1239. <http://dx.doi.org/10.1016/j.lwt.2010.03.014>.
- Escamilla-García, M., Calderon-Dominguez, G., Chanona-Perez, J. J., Farrera-Rebollo, R. R., Andraca-Adame, J. A., Arzate-Vazquez, I., Mendez-Mendez, J. V., & Moreno-Ruiz, L. A. (2013). Physical and structural characterisation of zein and chitosan edible films using nanotechnology tools. *International Journal of Biological Macromolecules*, 61, 196-203. <http://dx.doi.org/10.1016/j.ijbiomac.2013.06.051>. PMID:23831381.
- Ferreira, A. R. V., Bandarra, N. M., Moldão-Martins, M., Coelho, I. M., & Alves, V. D. (2018). FucoPol and chitosan bilayer films for walnut kernels and oil preservation. *Lebensmittel-Wissenschaft + Technologie*, 91, 34-39. <http://dx.doi.org/10.1016/j.lwt.2018.01.020>.
- Gutiérrez, T. J., Morales, N. J., Pérez, E., Tapia, M. S., & Famá, L. (2015). Physico-chemical properties of edible films derived from native and phosphated cush-cush yam and cassava starches. *Food Packaging Shelf*, 3, 1-8. <http://dx.doi.org/10.1016/j.fpsl.2014.09.002>.
- Haghighi, H., De Leo, R., Bedin, E., Pfeifer, F., Siesler, H. W., & Pulvirenti, A. (2019). Comparative analysis of blend and bilayer films based

- on chitosan and gelatin enriched with LAE (lauroyl arginate ethyl) with antimicrobial activity for food packaging applications. *Food Packaging Shelf*, 19, 31-39. <http://dx.doi.org/10.1016/j.fpsl.2018.11.015>.
- Hahladakis, J. N., Velis, C. A., Weber, R., Iacovidou, E., & Purnell, P. (2018). An overview of chemical additives present in plastics: migration, release, fate and environmental impact during their use, disposal and recycling. *Journal of Hazardous Materials*, 344, 179-199. <http://dx.doi.org/10.1016/j.jhazmat.2017.10.014>. PMID:29035713.
- Jridi, M., Abdelhedi, O., Zouari, N., Fakhfakh, N., & Nasri, M. (2019). Development and characterization of grey triggerfish gelatin/agar bilayer and blend films containing vine leaves bioactive compounds. *Food Hydrocolloids*, 89, 370-378. <http://dx.doi.org/10.1016/j.foodhyd.2018.10.039>.
- Koshy, R. R., Mary, S. K., Thomas, S., & Pothan, L. A. (2015). Environment friendly green composites based on soy protein isolate-A review. *Food Hydrocolloids*, 50, 174-192. <http://dx.doi.org/10.1016/j.foodhyd.2015.04.023>.
- Leonardo, M. F., & Jonas, T. G. (2020). Whey protein films added with galactooligosaccharide and xylooligosaccharide. *Food Hydrocolloids*, 104, 105755. <http://dx.doi.org/10.1016/j.foodhyd.2020.105755>.
- Liang, J., Yan, H., Wang, X., Zhou, Y., Gao, X., Puligundla, P., & Wan, X. C. (2017). Encapsulation of epigallocatechin gallate in zein/chitosan nanoparticles for controlled applications in food systems. *Food Chemistry*, 231, 19-24. <http://dx.doi.org/10.1016/j.foodchem.2017.02.106>. PMID:28449996.
- López, O. V., Versino, F., Villar, M. A., & Garcia, M. A. (2015). Agro-industrial residue from starch extraction of *Pachyrhizus ahipa* as filler of thermoplastic corn starch films. *Carbohydrate Polymers*, 134, 324-332. <http://dx.doi.org/10.1016/j.carbpol.2015.07.081>. PMID:26428131.
- Lopez, O., Garcia, M. A., Villar, M. A., Gentili, A., Rodriguez, M. S., & Albertengo, L. (2014). Thermo-compression of biodegradable thermoplastic corn starch films containing chitin and chitosan. *Lebensmittel-Wissenschaft + Technologie*, 57(1), 106-115. <http://dx.doi.org/10.1016/j.lwt.2014.01.024>.
- Mathew, S., Brahmakumar, M., & Abraham, T. E. (2006). Microstructural imaging and characterization of the mechanical, chemical, thermal, and swelling properties of starch-chitosan blend films. *Biopolymers*, 82(2), 176-187. <http://dx.doi.org/10.1002/bip.20480>. PMID:16489584.
- Mendes, J. F., Paschoalin, R. T., Carmona, V. B., Sena Neto, A. R., Marques, A. C. P., Marconcini, J. M., Mattoso, L. H. C., Medeiros, E. S., & Oliveira, J. E. (2016). Biodegradable polymer blends based on corn starch and thermoplastic chitosan processed by extrusion. *Carbohydrate Polymers*, 137, 452-458. <http://dx.doi.org/10.1016/j.carbpol.2015.10.093>. PMID:26686150.
- Niluwan, K., Benjakul, S., & Prodpran, T. (2018). Physical/thermal properties and heat seal ability of bilayer films based on fish gelatin and poly (lactic acid). *Food Hydrocolloids*, 77, 248-256. <http://dx.doi.org/10.1016/j.foodhyd.2017.10.001>.
- Niluwan, K., Benjakul, S., Prodpran, T., & de la Caba, K. (2019). Fish gelatin monolayer and bilayer films incorporated with epigallocatechin gallate: Properties and their use as pouches for storage of chicken skin oil. *Food Hydrocolloids*, 89, 783-791. <http://dx.doi.org/10.1016/j.foodhyd.2018.11.056>.
- Ninago, M. D., López, O. V., Lencina, M. S., García, M. A., Andreucetti, N. A., Ciolino, A. E., & Villar, M. A. (2015). Enhancement of thermoplastic starch final properties by blending with poly (ϵ -caprolactone). *Carbohydrate Polymers*, 134, 205-212. <http://dx.doi.org/10.1016/j.carbpol.2015.08.007>. PMID:26428117.
- Nur Hanani, Z. A., Aelma Husna, A. B., Nurul Syahida, S., Nor Khaizura, M. A. B., & Jamilah, B. (2018). Effect of different fruit peels on the functional properties of gelatin/polyethylene bilayer films for active packaging. *Food Packaging Shelf*, 18, 201-211. <http://dx.doi.org/10.1016/j.fpsl.2018.11.004>.
- Ren, L., Yan, X., Zhou, J., Tong, J., & Su, X. (2017). Influence of chitosan concentration on mechanical and barrier properties of corn starch/chitosan films. *International Journal of Biological Macromolecules*, 105(Pt 3), 1636-1643. <http://dx.doi.org/10.1016/j.ijbiomac.2017.02.008>. PMID:28167105.
- Santoso, B., Hazirah, R., Priyanto, G., Hermanto, D., & Sugito, D. (2019). Utilization of *Uncaria gambir* Roxb filtrate in the formation of bioactive edible films based on corn starch. *Food Sci. Technol.*, 39(4), 837-842. <http://dx.doi.org/10.1590/fst.06318>.
- Scaffaro, R., Sutera, F., & Botta, L. (2018). Biopolymeric bilayer films produced by co-extrusion film blowing. *Polymer Testing*, 65, 35-43. <http://dx.doi.org/10.1016/j.polymertesting.2017.11.010>.
- Shahbazi, M., Rajabzadeh, G., & Ahmadi, S. J. (2017). Characterization of nanocomposite film based on chitosan intercalated in clay platelets by electron beam irradiation. *Carbohydrate Polymers*, 157, 226-235. <http://dx.doi.org/10.1016/j.carbpol.2016.09.018>. PMID:27987922.
- Silva, M. A., Bierhalz, A. C. K., & Kieckbusch, T. G. (2009). Alginate and pectin composite films crosslinked with Ca²⁺ ions: Effect of the plasticizer concentration. *Carbohydrate Polymers*, 77(4), 736-742. <http://dx.doi.org/10.1016/j.carbpol.2009.02.014>.
- Sogut, E., & Seydim, A. C. (2018). Development of Chitosan and Polycaprolactone based active bilayer films enhanced with nanocellulose and grape seed extract. *Carbohydrate Polymers*, 195, 180-188. <http://dx.doi.org/10.1016/j.carbpol.2018.04.071>. PMID:29804967.
- Sogut, E., & Seydim, A. C. (2019). The effects of chitosan-and polycaprolactone-based bilayer films incorporated with grape seed extract and nanocellulose on the quality of chicken breast fillets. *Lebensmittel-Wissenschaft + Technologie*, 101, 799-805. <http://dx.doi.org/10.1016/j.lwt.2018.11.097>.
- Soliman, E. A., Khalil, A. A., Deraz, S. F., El-Fawal, G., & Elrahman, S. A. (2014). Synthesis, characterization and antibacterial activity of biodegradable films prepared from Schiff bases of zein. *Journal of Food Science and Technology*, 51(10), 2425-2434. <http://dx.doi.org/10.1007/s13197-012-0792-y>. PMID:25328181.
- Song, X. Y., Cheng, L. Y., & Tan, L. (2018a). Edible iron yam and maize starch convenient food flavoring packaging films with lemon essential oil as plasticization. *Food Sci. Technol.*, 39(4), 971-979. <http://dx.doi.org/10.1590/fst.13118>.
- Song, X., Zuo, G., & Chen, F. (2018b). Effect of essential oil and surfactant on the physical and antimicrobial properties of corn and wheat starch films. *International Journal of Biological Macromolecules*, 107(Pt A), 1302-1309. <http://dx.doi.org/10.1016/j.ijbiomac.2017.09.114>. PMID:28970166.
- Soo, P. Y., & Sarbon, N. M. (2018). Preparation and characterization of edible chicken skin gelatin film incorporated with rice flour. *Food Packaging Shelf*, 15, 1-8. <http://dx.doi.org/10.1016/j.fpsl.2017.12.009>.
- Sun, H., Shao, X., Jiang, R., Shen, Z., & Ma, Z. (2018). Mechanical and barrier properties of corn distarch phosphate-zein bilayer films by thermocompression. *International Journal of Biological Macromolecules*, 118(Pt B), 2076-2081. <http://dx.doi.org/10.1016/j.ijbiomac.2018.07.069>. PMID:30009915.
- Thu, H. E., Zulfakar, M. H., & Ng, S. F. (2012). Alginate based bilayer hydrocolloid films as potential slow-release modern wound dressing. *International Journal of Pharmaceutics*, 434(1-2), 375-383. <http://dx.doi.org/10.1016/j.ijpharm.2012.05.044>. PMID:22643226.

- Turner, A. (2018). Black plastics: linear and circular economies, hazardous additives and marine pollution. *Environment International*, 117, 308-318. <http://dx.doi.org/10.1016/j.envint.2018.04.036>. PMID:29778831.
- Valencia-Sullca, C., Vargas, M., Atarés, L., & Chiralt, A. (2018). Thermoplastic cassava starch-chitosan bilayer films containing essential oils. *Food Hydrocolloids*, 75, 107-115. <http://dx.doi.org/10.1016/j.foodhyd.2017.09.008>.
- Wang, H., Gong, X., Miao, Y., Guo, X., Liu, C., Fan, Y. Y., Zhang, J., Niu, B. L., & Li, W. (2019). Preparation and characterization of multilayer films composed of chitosan, sodium alginate and carboxymethyl chitosan-ZnO nanoparticles. *Food Chemistry*, 283, 397-403. <http://dx.doi.org/10.1016/j.foodchem.2019.01.022>. PMID:30722890.
- Wang, W., Wang, K., Xiao, J., Liu, Y., Zhao, Y., & Liu, A. (2017). Performance of high amylose starch-composited gelatin films influenced by gelatinization and concentration. *International Journal of Biological Macromolecules*, 94(Pt A), 258-265. <http://dx.doi.org/10.1016/j.ijbiomac.2016.10.014>. PMID:27732878.
- Xin, Y., Jin, Z., Chen, F., Lai, S., & Yang, H. (2020). Effect of chitosan coatings on the evolution of sodium carbonate-soluble pectin during sweet cherry softening under non-isothermal conditions. *International Journal of Biological Macromolecules*, 154, 267-275. <http://dx.doi.org/10.1016/j.ijbiomac.2020.03.104>. PMID:32179112.
- Yalçinkaya, S., & Çakmak, D. (2017). Electrochemical synthesis of poly (pyrrole-co-o-anisidine) /chitosan composite films. *Journal of Molecular Structure*, 1135, 32-43. <http://dx.doi.org/10.1016/j.molstruc.2017.01.040>.
- Zhang, L., Chen, F., Lai, S., Wang, H., & Yang, H. (2018). Impact of soybean protein isolate-chitosan edible coating on the softening of apricot fruit during storage. *Lebensmittel-Wissenschaft + Technologie*, 96, 604-611. <http://dx.doi.org/10.1016/j.lwt.2018.06.011>.
- Zhang, Y. Z., Li, J., Zhao, J., Bian, W., Li, Y., & Wang, X. J. (2016). Adsorption behavior of modified Iron stick yam skin with Polyethyleneimine as a potential biosorbent for the removal of anionic dyes in single and ternary systems at low temperature. *Bioresource Technology*, 222, 285-293. <http://dx.doi.org/10.1016/j.biortech.2016.09.108>. PMID:27723475.
- Zhu, J. Y., Tang, C. H., Yin, S. W., & Yang, X. Q. (2018). Development and characterization of novel antimicrobial bilayer films based on Polylactic acid (PLA)/Pickering emulsions. *Carbohydrate Polymers*, 181, 727-735. <http://dx.doi.org/10.1016/j.carbpol.2017.11.085>. PMID:29254029.
- Zhuang, C., Jiang, Y., Zhong, Y., Zhao, Y., Deng, Y., Yue, J., Wang, D., Jiao, S., Gao, H., Chen, H., & Mu, H. (2018). Development and characterization of nano-bilayer films composed of polyvinyl alcohol, chitosan and alginate. *Food Control*, 86, 191-199. <http://dx.doi.org/10.1016/j.foodcont.2017.11.024>.